

Radiation Absorption Coefficients of Polycrystalline Ice From 400-1400 nm

THOMAS C. GRENFELL AND DONALD K. PEROVICH

Department of Atmospheric Sciences AK-40, University of Washington, Seattle, Washington 98195

Absorption coefficients have been measured for bubble-free polycrystalline ice over the spectral region 400-1400 nm. In order to obtain an easily measurable attenuation at short wavelengths (400-500 nm), a 2.83 m block was used. The technique employed to grow large quantities of bubble-free ice is presented in detail. The absorption coefficients agree very well with previous results in the infrared and appear to provide greater accuracy and spectral detail at visible wavelengths.

INTRODUCTION

Although pure ice is highly transparent at visible wavelengths, absorption of solar radiation by naturally occurring forms of ice is far from negligible at these wavelengths. Because natural ice forms usually contain considerable quantities of internal inhomogeneities or consist of small crystals or granules, substantial volume scattering takes place and greatly increases the effective path length of photons through the medium so that extinction becomes very large. This has been demonstrated for glacier ice and snow by *Ambach and Habicht* [1962], and for sea ice by *Grenfell and Maykut* [1977]. Consequently, for a variety of studies related to the radiative energy balance of the earth's surface in cold regions, an accurate knowledge of the spectral absorption coefficients of pure bubble-free ice [k_λ (ice)] is needed. For example, recent calculations of spectral albedos and extinction coefficients of snow [*Bohren and Barkstrom*, 1974; *Choudhury and Chang*, 1979; *Wiscombe and Warren*, 1980], transmissivities and reflectances of ice clouds [*Liou*, 1973], and optical properties of sea ice [*Grenfell*, 1979] all depend on k_λ (ice). In addition, photometric models of planetary atmospheres and snow or ice-covered extraterrestrial objects require accurate data on the spectral properties of ice [*Van de Hulst and Irvine*, 1962; *Sagan and Pollack*, 1967].

Over the visible region the best available results of ice transparency are those of *Sauberer* [1950]. They have been cited by *Goodrich* [1970] and presented by him in terms of spectral absorption coefficients. The uncertainties in these data are substantial because a very large length of pure bubble-free ice is necessary to obtain a sufficient path length to get a dependably measurable attenuation, but large enough quantities of bubble-free ice are difficult to obtain. Even if a large quantity of ice is available, scattering from crystal boundaries can be significant. For the most part, *Sauberer* [1950] used samples from 14 to 16 cm in thickness although a few of his samples were as long as 50 cm. The total absorption thus ranged from 0.4% to 2% requiring very stable electronics for even moderate accuracy. It is not surprising then that his results appear to have been somewhat noisy although he gives no quantitative error estimates. Accordingly, *Goodrich* [1970] quotes *Sauberer's* visible results to at most two significant figures.

In the infrared, data are available from several sources and because absorption is greater, there is a corresponding increase in accuracy for small sample sizes. Recent reviews [*Ir-*

vine and Pollack, 1968; *Goodrich*, 1970; *Wiscombe and Warren*, 1980] have shown, however, that a good deal of subjective evaluation and interpolation are still necessary to provide continuity of k_λ (ice) over a wide spectral range. This probably arises from difficulties in sample preparation, but may also be due to detector sensitivity limitations or light leakage problems in some spectral regions.

The goal of the present study has been to obtain continuous values of k_λ (ice) over the visible and near infrared with improved absolute accuracy and spectral resolution. This has been made possible by the adaptation of a simple technique for growing large quantities of pure bubble-free ice together with the availability of a very wide band visible and infrared scanning photometer [*Grenfell*, 1981].

SAMPLE PREPARATION

The method used for growing bubble-free ice was developed in our laboratory by D. Bell et al. (unpublished data, 1972). The ice was grown in a tank with foam insulated plexiglas walls, a styrofoam lid, and a bottom surface of aluminum chosen for its high thermal conductivity. The tank was placed in a cold room set at +2°C, and a network of copper cooling coils was installed underneath it in contact with the aluminum bottom so that the ice would grow upward from the bottom of the tank. The apparatus is shown in Figure 1. The tank was carefully cleaned and filled with filtered deionized water. As ice growth proceeded, the water was circulated over the growing surface using stirring motors mounted on the lid in order to dislodge bubbles nucleating on the growing surface and to keep any particulates in the water in motion so they would not freeze into the ice. Periodically the water was siphoned off to remove the small amounts of dust which had accumulated and prevent any buildup of chemical impurities. The growth time was slow to promote large crystal growth; 200 mm of ice was grown over a 10 day period.

The sample produced was a rectangular block 2.83 m in length and 260 × 200 mm in width and height. This length was chosen to give a total absorption at 400-500 nm of about 10% based on the data of *Sauberer* [1950]. The ends of the tank were smooth 15.9 mm (5/8") thick plexiglas which were removed after the block had finished growing leaving flat optically smooth surfaces. One end face of the tank was tilted at 10° to remove effects of multiple internal reflections.

MEASUREMENTS

The experimental setup is shown in Figure 2. A collimated beam of light was directed through the sample, its intensity was measured using the scanning photometer whose operating

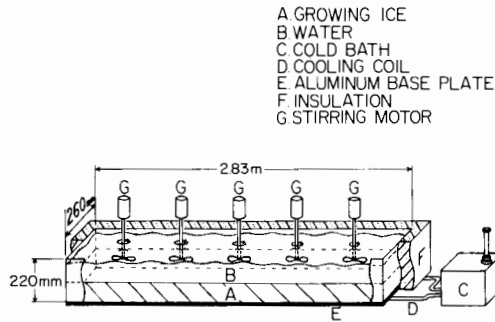


Fig. 1. Schematic representation of the ice growth apparatus (not to scale).

characteristics are described by Grenfell [1981], and the output versus wavelength was recorded on an x - y plotter. The ice block was then removed and the measurement repeated. Each time the ice block was moved, the light source and the photometer were realigned to give a maximum reading. Because k_λ (ice) changes by 6 orders of magnitude over the wavelength range studied, blocks of three different lengths were used to optimize accuracy in different wavelength regions. The appropriate block sizes were estimated using Sauberer's data. The full 2.83 m block was used from 400 to 850 nm. For the near infrared from 700 to 1100 nm a 200 mm section was cut from the full block, and for the 1000 to 1400 nm region an additional 8.2 mm thick slab was cut. The end faces of the smaller blocks were melted flat using an aluminum plate, and polished with a soft cloth.

Two light sources were used. The first was a standard slide projector from which the infrared blocking filter could be removed when necessary. The cross sectional area of the projector beam was then restricted with light baffles to 30×30 mm before it entered the ice. For reference, a helium-neon laser was also used because of its narrow collimated beam and its precisely known wavelength and narrow bandpass.

Because of the polycrystalline nature of the ice, some volume scattering was inevitable. Because the individual crystals were vertical columns, the scattering was horizontal, so the experiment was designed to measure all light including that scattered out of the beam. Visual inspection showed that apart from Fresnel reflection at the ends of the block, side and backscattering were negligible; thus virtually no light escaped out the sides of the block. Small angle forward scattering was observed as expected in the 2.83 m block, but was negligible in the smaller samples. Consequently, two different detector

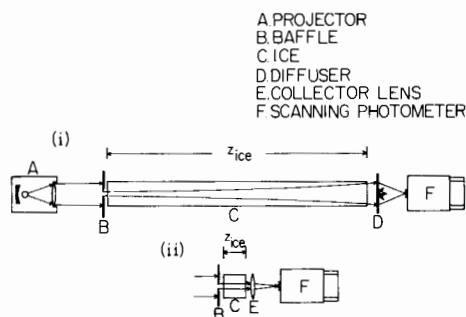


Fig. 2. Schematic representation in plan view of the setup for the optical measurements. Configuration (i) was used for the full 2.83 m block and configuration (ii) for the shorter samples.

configurations were used. At visible wavelengths, a 3.2 mm ($1/8$ "") thick opal plexiglas diffusing plate was mounted perpendicular to the incident beam 30 cm in front of the photometer as shown in Figure 2*i*. This made it possible to sample all the light passing through the end of the block eliminating internal scattering losses. At infrared wavelengths, absorption by the plexiglas was too strong to obtain an adequate signal to noise ratio; but, because the block size was small and the scattering negligible, it was possible to focus the entire emerging beam onto the entrance aperture of the photometer by using a collector lens as shown in Figure 2*ii*.

Frost formation was a problem when the air outside the cold room was humid. In such cases, care was taken to polish the ends of the sample clean just before the measurements were taken, and multiple scans were recorded to test for signal degradation due to subsequent frost buildup.

Absorption coefficients were calculated using the following formula for attenuation in purely absorbing media:

$$k_\lambda(\text{ice}) = -\frac{1}{z_{\text{ice}}} \ln \{I_\lambda(\text{ice})/[I_\lambda(\text{no ice})(1 - r_\lambda^f)(1 - r_\lambda^b)]\}$$

where z_{ice} is the length of the sample, $I_\lambda(\text{ice/no ice})$ is the observed light intensity with/without the ice in place, and $r_\lambda^{f/b}$ is the calculated Fresnel reflection loss for the front or back surface. The results are displayed graphically in Figure 3 and are given in Table 1 at 10 nm intervals. Table 1 also contains the corresponding values of the imaginary part of the index of refraction (n_{im}) calculated from $n_{im} = \lambda k_\lambda(\text{ice})/4\pi$ [Born and Wolf, 1959].

Observational uncertainties listed in Table 1 and shown in Figure 3 include the following sources: instrumental noise, repeatability of the intensity observations, and uncertainty in measuring z_{ice} . The latter was significant only for the 8.2 mm thick slab. The influence of multiple internal reflections on the results was calculated and found to be negligible. In order to insure continuity in the regions of overlap between different

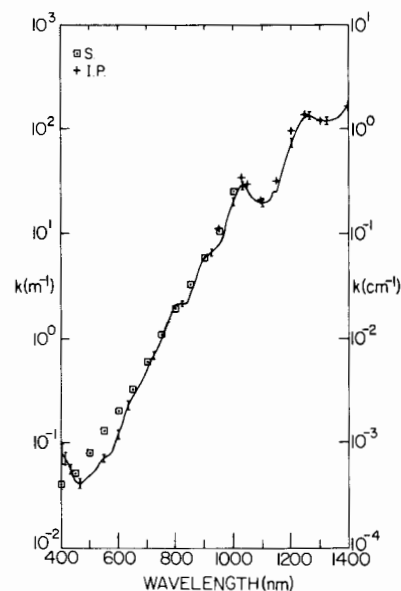


Fig. 3. The absorption coefficient of ice versus wavelength. The solid curve shows the present results together with the error estimates. The boxed dots show the data points of Sauberer (S.) and the crosses show the data from Irvine and Pollack (I.P.).

TABLE 1. Absorption Coefficients and Corresponding Imaginary Components of the Index of Refraction for Pure Bubble-Free Ice

λ , nm	k , m^{-1}	n_{im}	Uncertainty, %
400	8.50E - 2	2.71E - 9	± 20
10	7.70	2.51	± 19
20	6.77	2.26	± 18
30	6.09	2.08	± 12
40	5.45	1.91	± 11
450	4.30E - 2	1.54E - 9	± 10
60	4.19	1.53	
70	4.14	1.55	
80	4.30	1.64	
90	4.57	1.78	
500	4.79E - 2	1.91E - 9	± 10
10	5.26	2.14	
20	5.45	2.26	
30	6.03	2.54	
40	6.83	2.93	
550	7.10E - 2	3.11E - 9	± 10
60	7.38	3.29	
70	7.75	3.52	
80	8.76	4.04	
90	1.04E - 1	4.88	
600	1.20E - 1	5.73E - 9	± 10
10	1.42	6.89	
20	1.74	8.58	
30	2.08	1.04E - 8	
40	2.40	1.22	
650	2.76E - 1	1.43E - 8	± 10
60	3.16	1.66	
70	3.54	1.89	
80	3.86	2.09	
90	4.38	2.40	
700	5.20E - 1	2.90E - 8	± 8
10	6.09	3.44	
20	7.03	4.03	
30	7.41	4.30	
40	8.35	4.92	
750	9.84E - 1	5.87E - 8	± 8
60	1.17E - 0	7.08	
70	1.40	8.58	
80	1.64	1.02E - 7	
90	1.87	1.18	
800	2.10E - 0	1.34E - 7	± 8
10	2.17	1.40	
20	2.19	1.43	
30	2.19	1.45	
40	2.26	1.51	
850	2.70E - 0	1.83E - 7	± 8
60	3.14	2.15	
70	3.83	2.65	
80	4.78	3.35	
90	5.53	3.92	
900	5.86E - 0	4.20E - 7	± 8
10	6.13	4.44	
20	6.48	4.74	
30	6.90	5.11	
40	7.39	5.53	
950	7.96E - 0	6.02E - 7	± 8
60	9.88	7.55	
70	1.20E + 1	9.26	
80	1.43	1.12E - 6	
90	1.69	1.33	
1000	2.04E + 1	1.62E - 6	± 10
10	2.49	2.00	
20	2.77	2.25	
30	2.84	2.33	
40	2.81	2.33	
1050	2.60E + 1	2.17E - 6	± 10
60	2.32	1.96	
70	2.12	1.81	
80	2.03	1.74	
90	1.99	1.73	
1100	1.94E + 1	1.70E - 6	± 10
10	1.99	1.76	

TABLE 1. (continued)

λ , nm	k , m^{-1}	n_{im}	Uncertainty, %
20	2.04	1.82	
30	2.27	2.04	
40	2.48	2.25	
1150	2.50E + 1	2.29E - 6	± 10
60	3.29	3.04	
70	4.12	3.84	
80	5.08	4.77	
90	6.08	5.76	
1200	7.03E + 1	6.71E - 6	± 10
10	8.99	8.66	
20	1.05E + 2	1.02E - 5	
30	1.15	1.13	
40	1.24	1.22	
1250	1.30E + 2	1.29E - 5	± 10
60	1.32	1.32	
70	1.34	1.35	
80	1.31	1.33	
90	1.29	1.32	
1300	1.28E + 2	1.32E - 5	± 10
10	1.26	1.31	
20	1.26	1.32	
30	1.25	1.32	
40	1.26	1.34	
1350	1.29E + 2	1.39E - 5	± 10
60	1.31	1.42	
70	1.36	1.48	
80	1.44	1.58	
90	1.57	1.74	
1400	1.78E + 2	1.98E - 5	± 10

scans, small adjustments were applied to the measured radiances within the limits of observational uncertainty.

After the optical measurements had been completed, vertical and horizontal thin sections were prepared and the crystal structure of the ice was examined under crossed polaroids. The block consisted of an array of columnar crystals extending the full height of the tank (200 mm). The typical horizontal extent of a single crystal was 50–100 mm and the largest observed was 80 \times 200 mm. The thin sections were then examined under a microscope to look for bubbles and other inclusions. Individual bubbles down to 1 micron in diameter could be detected easily. In 3×10^6 mm³ of ice inspected, only three bubbles were found (near the edge of one sample) suggesting a density on the order of 10^{-6} mm³ or less. Several smaller volumes of ice were examined very carefully to look for clusters of bubbles or indications of cloudiness at the limit of resolution and none were found. No trace of inclusions of any other sort was detected.

DISCUSSION

For comparison with the present results, the data of Sauberer [1950] from 400 to 1000 nm as presented by Goodrich [1970] together with the values from 950 to 1400 nm compiled by Irvine and Pollack [1968] are included in Figure 3. From 1050 to 1400 nm the agreement with previous data is very good, but differences appear gradually at shorter wavelengths and are greatest between 400 and 600 nm. Because of the greater path length and improved spectral resolution, the present results are felt to be more accurate than those of Sauberer [1950]. However, in view of the stated limitations in

Sauberer's data, his results are felt to be surprisingly close to the present values, and within the limits of his uncertainties, the two data sets are probably consistent with one another.

Additional arguments qualitatively supporting the present results can also be made from a comparison with the absorption coefficients of pure water where large path lengths are easier to obtain. Values of k_λ (water) are reported by Irvine and Pollack [1968]. They show that between 900 and 3000 nm equivalent spectral features occur for both ice and water, but those for ice are shifted to slightly longer wavelengths presumably due to lattice interaction energies in ice. The present data continue this trend to shorter wavelengths. The features observed for water, a dip from 750 to 850 nm and a slight shoulder between 850 and 900 nm, are found for ice at 800–840 nm and 900–950 nm, respectively. The minimum for ice appears at 470 nm which is right at the minimum for water quoted by Irvine and Pollack. More recent measurements by Tyler and Smith [1970], however, suggest that the minimum occurs closer to 430 nm for pure natural water. Although there is no guarantee that the relationships between the results for ice and water which hold in the infrared should still be valid at visible wavelengths, it is reassuring to see that this indeed appears to be the case.

Acknowledgments. We would like to express our sincere thanks to David Bell for his help in producing the ice and assisting with the measurements. We are also indebted to Peter Kauffman for assistance with the photometer electronics and to the Office of Naval Research for financial support under contract N00014-76-C-0234. Atmospheric Sciences contribution 577.

REFERENCES

Ambach, W., and H. L. Habicht, Untersuchungen der Extinctionseigenschaften des Gletchereises und Schnees (Studies of

- the extinction properties of glacier ice and snow), *Arch. Meteorol. Geophys. Bioklimatol.*, 11(4), 512–532, 1962.
- Bohren, C. F., and B. R. Barkstrom, Theory of the optical properties of snow, *J. Geophys. Res.*, 79, 4527–4535, 1974.
- Born, M., and E. Wolf, *Principles of Optics*, 3rd ed., 808 pp., Pergamon, New York, 1959.
- Choudhury, B. J., and A. T. C. Chang, Two-stream theory of reflectance of snow, *IEEE Trans. Geosci. Electron.*, GE-17, 63–68, 1979.
- Goodrich, L. E., Review of radiation absorption coefficients for clear ice in the spectral region 0.3 to 3 microns, *Tech. Pap. 331*, 14 pp., Nat. Res. Council Div. of Building Res., Ottawa, 1970.
- Grenfell, T. C., The effects of ice thickness on the exchange of solar radiation over the polar oceans, *J. Glaciol.*, 22, 305–320, 1979.
- Grenfell, T. C., A visible and near infrared scanning photometer for field measurements of spectral albedo and irradiance under polar conditions, *J. Glaciol.*, in press, 1981.
- Grenfell, T. C., and G. A. Maykut, The optical properties of ice and snow in the Arctic Basin, *J. Glaciol.*, 18, 445–463, 1977.
- Irvine, W. M., and J. B. Pollack, Infrared optical properties of water and ice spheres, *Icarus*, 8, 324–360, 1968.
- Liou, K. N., Transfer of solar irradiance through cirrus cloud layers, *J. Geophys. Res.*, 78, 1409–1418, 1973.
- Sagan, C., and J. B. Pollack, Anisotropic nonconservative scattering and the clouds of Venus, *J. Geophys. Res.*, 72, 469–477, 1967.
- Sauberer, F., Die spektrale Strahlungsdurchlässigkeit des Eises (The spectral transparency of ice), *Wetter Leben*, 2(9/10), 193–197, 1950.
- Tyler, J. E., and R. C. Smith, *Measurements of Spectral Irradiance Underwater*, 1st ed., 103 pp., Gordon and Breach, New York, 1970.
- Van de Hulst, H. C., and W. M. Irvine, General report on radiation transfer in planets: Scattering in model planetary atmospheres, in *La Physique des Planètes, Proc. XI Intern. Astrophys. Symp.*, pp. 78–98, Univ. of Liège, Liège, Belgium, 1962.
- Wiscombe, W. J., and S. G. Warren, A model for the spectral albedo of snow, I, Pure snow, *J. Atmos. Sci.*, 37, 2712–2733, 1980.

(Received November 17, 1980;
revised February 19, 1981;
accepted February 23, 1981.)